

Model Predictive Control of a Fixed-Bed Reactor with Nonlinear Quality Inference

In Sik Chin, Jin Won Chung and Kwang Soon Lee[†]

Department of Chem. Eng., Sogang Univ., Shinsoo-1, Mapogu, Seoul 121-742, Korea

(Received 9 August 2001 • accepted 3 December 2001)

Abstract—A generic model predictive control framework has been proposed for a fixed-bed reactor with exothermic reaction. The proposed framework can conduct nonlinear inferential control of a product concentration together with linear multivariable control of bed temperatures. In addition, the framework can accommodate the multi-rate sampling and analysis delay caused by the product measurement. Performance of the proposed technique has been demonstrated with a non-adiabatic fixed bed reactor model producing maleic anhydride under various operating scenarios.

Key words: Model Predictive Control, Quality Control, Inferential Control, Reactor Control, Fixed-Bed Reactor

INTRODUCTION

Among many different types of reactors that play important roles in chemical plants, the non-adiabatic fixed-bed reactor with exothermic reactions has drawn constant interests from many researchers. One of the reasons for this is the sensitive and intricate characteristics of the reactor system caused by the heat of reaction nonlinearly dependent on the bed-temperature [Cho et al., 1998]. Such characteristics may destabilize the reactor system and thus have posed interesting operational problems on bed temperature control. It is well-known that the hot spot is most sensitive to changes in operating conditions. The industrial practice has been to pick the highest one among the multiple temperature measurements placed at various axial positions and regulate it. However, the temperature does not necessarily represent the hot spot since the hot spot may occur between sensing positions and moreover may drift along the axial direction depending on the operating conditions. A refined method to locate the hot spot more precisely would improve the temperature control aspect of the fixed-bed reactor.

While the hot spot temperature is an important control item for reactor stability, the product composition is the key item that determines the economy of the reactor operation. However, due to the limitation of the current process analyzers, on-line measurement of the product composition is available only with a long sampling interval with a long analysis delay. Another aspect to consider is that the product composition frequently appears as a highly nonlinear function of the operating conditions since the economic optimum generally exists around an extremum point. For effective regulation of the product composition, therefore, nonlinear inferential control is required.

Addressing the above mentioned problems in full or in part, various control system designs have been studied. Perhaps Jutan et al. [1977] are one of the earliest contributors who studied model-based multivariable control of a fixed-bed reactor. They applied standard LQG (linear quadratic gaussian) control to a pilot-scale butane hydrogenolysis reactor. They derived a state space model from the rigorous nonlinear reactor model using orthogonal collocation and de-

signed the state estimator and controller based on this model. The controlled variables were bed temperatures and product composition. However, the true hot spot temperature was not traced and inferential composition control was not devised. Lee and Lee [1985] have proposed an optimizing control scheme that maximizes the profit from a reactor operation. They demonstrated the performance of the scheme in a pilot-scale fixed bed reactor producing maleic anhydride. Kozub et al. [1987] also conducted experimental study in the same butane hydrogenolysis reactor. They designed LQ and internal model control (IMC) using an empirical transfer function model and regulated propane yield and butane conversion measured with a process gas chromatograph by manipulating of a bed temperature set point and hydrogen flow rate. Chen and Sun [1991] have compared the performance of various adaptive inferential control schemes through simulation study. They showed that nonlinear estimator-based control performs better than those based on linear estimators. However, the mathematical formulation of the controller is too complex to use in industries. Budman et al. [1992] have proposed robust inferential control schemes for a packed-bed reactor system while comparing various inferential control techniques. Through experimental study, they observed that a linear static inference model on the basis of partial least square technique shows satisfactory performance. However, it was observed that the linear inferential control shows performance limitation when the process variables deviate from the nominal operating region. Doyle et al. [1996] proposed a nonlinear control algorithm using feedback linearization for a packed-bed reactor. Their concern was hot spot dynamics described by a wave propagation model (first-order hyperbolic partial differential equation). Hua et al. [1998] have proposed an approach to estimate the unknown states and inlet disturbance using a nonlinear state observer for an autothermal packed-bed reactor under periodic operation. The state observer was derived from the fundamental reactor model. Hua and Jutan [2000] have approached with the algorithm that has cascade control scheme with a nonlinear model structure for the control of packed-bed reactor. They constructed nonlinear process model and then adjusted the reference value for controlled variable based on the nonlinear process model during operation. With the model, the unknown temperature state and inlet concentration were estimated by a nonlinear observer from only a few temperature measurements.

[†]To whom correspondence should be addressed.

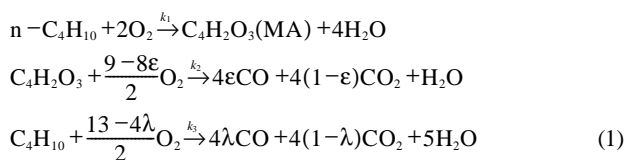
E-mail: kslee@ccs.sogang.ac.kr

The concern of the present study is placed on the practical and generic applicability of control schemes for fixed-bed reactors in addition to the performance. For this, we propose a generic model-based predictive control (MPC) framework for combined hot spot temperature control and nonlinear inferential control of product composition. This framework has advantages in that it can not only accommodate all the aspects and requirements of the non-adiabatic reactor mentioned previously but also handle various types of input and output constraints. In addition, all the necessary models for controller design are derived from data, which greatly reduces the modeling efforts compared to the fundamental model-based control schemes. The proposed control technique has been applied to a fixed-bed reactor model producing maleic anhydride (MA) by partial oxidation of n-butane (n-C4).

PROCESS DESCRIPTION

1. Numerical Modeling

We consider a non-adiabatic fixed-bed reactor producing MA from n-C4. The reaction is described by



Since the reactions are highly exothermic, suppression and effective removal of heat of reaction are paramount importance for stable and safe operation of the reactor. For this, n-C4 concentration in the feed stream is diluted at 1.2 vol% and the reactor is designed as a multi-tube heat exchanger with 1 inch inner diameter.

For this type of reactors, axial dispersion is negligible whereas the radial distributions of temperature and composition are important [Froment and Bischoff, 1979]. Under these assumptions, the pseudo-homogeneous two-dimensional reactor model can be set up.

Through a standard procedure, the mass and heat balance equations are represented as

$$\frac{\partial C_i}{\partial t} = -\left(\frac{1}{\tau\varepsilon}\right)\frac{\partial C_i}{\partial z} + \left(\frac{D_{er}}{R^2\varepsilon}\right)\frac{1}{r}\frac{\partial}{\partial r}\left(r\frac{\partial C_i}{\partial r}\right) + \frac{\rho_B}{\varepsilon}r_i \quad (2)$$

$$\frac{\partial T}{\partial t} = -\left(\frac{C_{pg}\rho_g}{\bar{C}\tau}\right)\frac{\partial T}{\partial z} + \left(\frac{k_{er}}{R^2\bar{C}}\right)\frac{1}{r}\frac{\partial}{\partial r}\left(r\frac{\partial T}{\partial r}\right) - \frac{\rho_B}{T_R\bar{C}}\sum_{j=1}^3\Delta h_j R_j \quad (3)$$

where

$$C_i = \frac{C_i^*}{C_R}, \quad r = \frac{r^*}{R}, \quad z = \frac{z^*}{L}, \quad \tau = \frac{L}{v}, \quad R_j = k_{j0}\exp^{(-E_j/RT)}.$$

In the above, the subscripts $i=1$ and 2 represent n-C4 and MA, respectively and the superscript $*$ means an actual value. Also, r_i and R_j represent the reaction rate producing the component i and the reaction rate for the j^{th} reaction path in Eq. (1), respectively. All the reaction rates are assumed to be of first-order.

The boundary and initial conditions are given by

$$\text{at } r=0, \quad \frac{\partial C_i}{\partial r} = \frac{\partial T}{\partial r} = 0$$

$$\text{at } r=1, \quad \frac{\partial C_i}{\partial r} = 0, \quad \frac{\partial T}{\partial r} = B_i(T_w - T)$$

Table 1. Parameters of the reactor model

| Nominal input values | $\tau=1.2$ [sec], $T_w=430$ [°K] |
|------------------------------|---|
| Parameters for normalization | $L=70$ [cm], $R=1.3$ [cm], $T_R=727$ [°K], $C_R=5.8036\times 10^{-7}$ [mol/cm ³] |
| Parameters for reaction | $k_{10}=1.320\times 10^3$ [cm ³ /sec·gcat], $k_{20}=1.612\times 10^2$ [cm ³ /sec·gcat], $k_{30}=4.050\times 10^4$ [cm ³ /sec·gcat], $\Delta h_1=-311.6$ [Kcal/gmol], $\Delta h_2=-140.1$ [Kcal/gmol], $\Delta h_3=-451.7$ [Kcal/gmol], $E_1=11,720$ [cal/gmol °K], $E_2=9,840$ [cal/gmol °K], $E_3=19,070$ [cal/gmol °K] |
| Parameters for heat transfer | $B_i=12$, $C_{pg}=0.267$ [cal/g °K], $D_{er}=2.8$ [cm ² /sec], $k_{er}=1.30$ [g/cm ³], $\bar{C}=0.34$ [cal/cm ³ °K], $\varepsilon=0.47$, $\rho_B=1.30$ [g/cm ³], $\rho_g=4.20\times 10^{-4}$ [g/cm ³] |

$$\text{at } z=0, \quad C_1=C_{10}, \quad C_2=0, \quad T=T_0$$

$$\text{at } t=0, \quad C_i=C_i^*(r, z), \quad T=T^0(r, z) \quad (4)$$

For simplification, the outer surface temperature of the reactor wall, T_w , has no spatial distribution and directly manipulable.

For numerical modeling, pseudo-steady state assumption is introduced for the component balances, *i.e.*, $\partial C_i/\partial t=0$, first, and then orthogonal collocations along the axial as well as radial directions were introduced. The number of internal collocation points for the radial and axial collocations were three and seven, respectively. This results in a two sets of 21 algebraic equations (AE's) from Eq. (2) and 21 ordinary differential equations (ODE's) from Eq. (3). Since the resulting equations from both Eqs. (2) and (3) are linear in compositions, the composition terms in the ODE's can be completely eliminated by the AE's leaving 21 nonlinear ODE's with respect to the bed temperatures. Detailed collocation procedure can be found in Lee [1983].

In Table 1, we list the nominal operating conditions and the parameter values used in the model.

In the concerned reactor, the hot spot temperature and MA yield are two important items to be regulated: the former for reactor stabilization and the latter for economy. For this, the wall temperature, T_w , and the space time, τ , are assumed to be manipulated.

It is assumed that the MA yield is measured at every 10 min with 10 min of analysis delay.

2. Bed Temperature Dynamics and Hot Spot Measurement

In this subsection, the current industrial practice on reactor temperature control, where a bed temperature at a fixed position is regulated, is reassessed first and an improved technique to more precisely estimate the hot spot temperature is proposed.

In Fig. 1, we show the dynamic responses of the bed temperature at $z=0.25$ to two different step changes in space time. This location is a little bit right to the hot spot under the nominal operating condition. It can be seen that the temperature always decreases at new steady states irrespective of the direction of $\Delta\tau$.

The above nonlinear behavior can be expected if we consider the traveling pattern of the temperature profile to changes in τ as

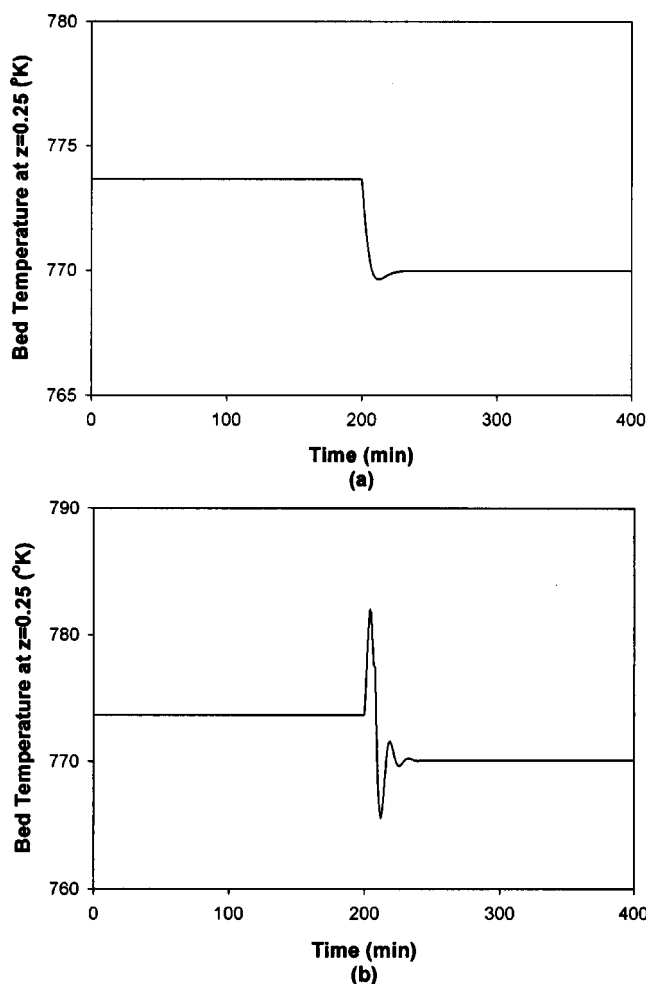


Fig. 1. Step response of temperature at $z=0.25$ when τ is increased by 20% (a) and τ is decreased by 50% (b).

depicted in Fig. 2. For example, to a increase in τ , $T(z=0.25)$ decreases monotonically. On the other hand, to a decrease in τ (Fig. 2b), $T(z=0.25)$ will increase and then decrease as the temperature profile moves backward along the axial direction, which may result in an inverse response. When the magnitude of the flow rate change is small, however, $T(z=0.25)$ may remain at a higher temperature than its initial value. In conclusion, a bed temperature at a fixed position not only cannot represent the true hot spot but also may raise difficulties in controller design. In industrial reactors of this type, it is common to fix the feed flow rate and only the jacket temperature is manipulated for bed-temperature control.

To improve the above problem, in this study, we trace and estimate the true hot spot. The bed temperature profile is approximated by a Lagrange interpolation polynomial determined using the bed temperature measurements and the hot spot is located where the first-order derivative of the polynomial vanishes.

Fig. 3 shows the step responses of the hot spot temperature. The nonlinearity problems can be observed in the figure. The steady state gains have the same sign for both positive and negative changes in the feed flow rate though some nonlinearities are observed during the transients. From the response, it can be easily expected that the linear controller may show the limitation in controlling the process.

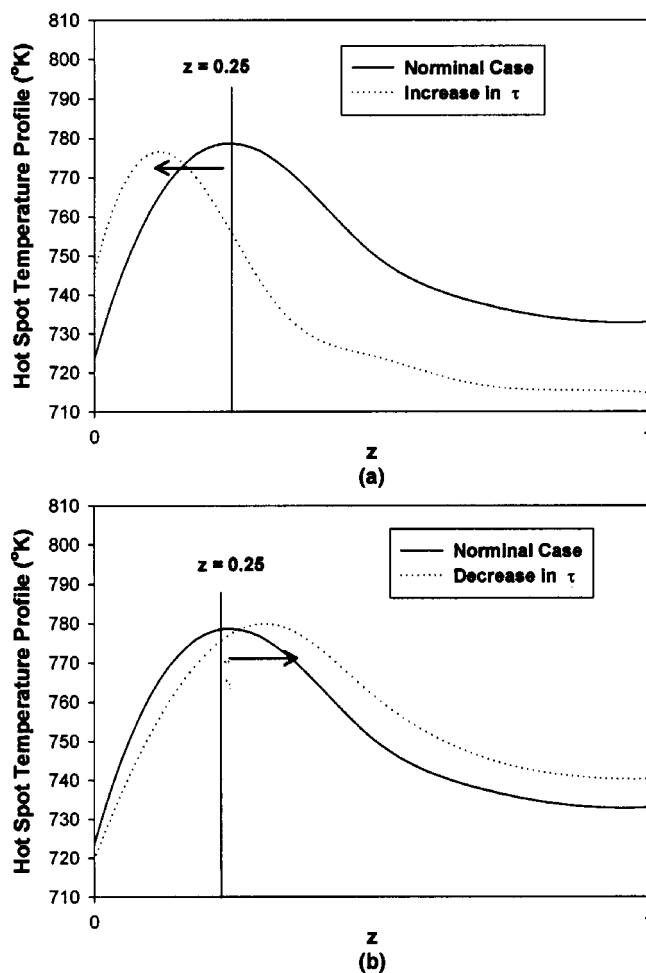


Fig. 2. Step response of hot spot temperature at when τ is increased by 20% (a) and τ is decreased by 50% (b).

With the proposed hot spot estimator, the overall reactor system with the associated input and output signals can be described as in Fig. 4. The sampling time for control was chosen to be 1 min.

DERIVATION OF THE CONTROL ALGORITHM

1. Model Development

For controller design, a linear state space model was introduced for the hot spot temperature. Since the hot spot temperature monotonically increases with the increase in the coolant temperature and remains almost unchanged with the change in residence time, this approach can be justified for a relatively large change in the hot spot temperature. If we let $y_T(t) \in \mathbb{R}$ and $u(t) \in \mathbb{R}^2$ denote the normalized deviation variables for the hot spot temperature and $[\tau \ T_w]^T$, respectively, the model is represented by

$$\begin{aligned} z(t+1) &= Az(t) + Bu(t) + v(t) \\ y_T(t) &= Cz(t) + w(t). \end{aligned} \quad (5)$$

where $v(t)$ and $w(t)$ are zero-mean white noise sequences. It is assumed the MA yield, $y_{MA}(t)$, can be related to the hot spot temperature and the input variable in the following quadratic form:

$$y_{MA}(t) = F_1 y_T(t) + F_2 u(t-1) + F_3 u^2(t-1) + r(t) \quad (6)$$

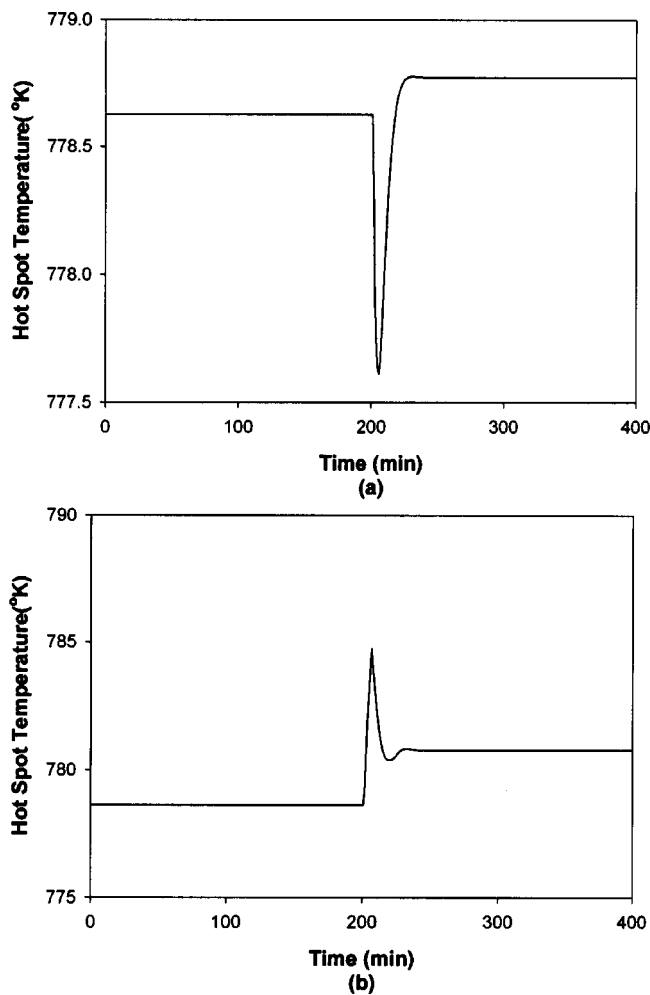


Fig. 3. Profile of reactor temperature when τ is increased by 20% (a) and τ is decreased by 50% (b).

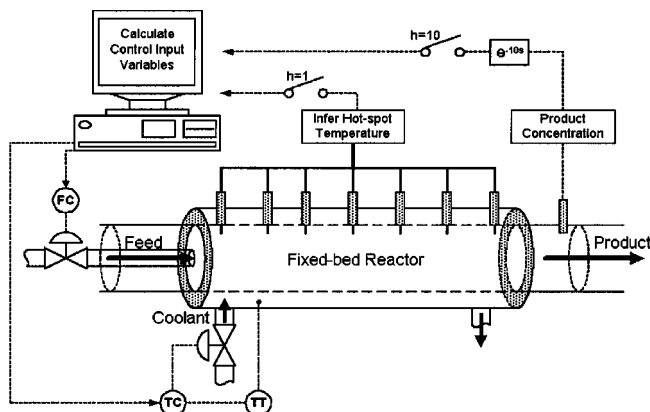


Fig. 4. Schematic diagram of the simulated reactor system.

where

$$u^2(t-1) \triangleq \begin{bmatrix} u_1^2(t-1) \\ u_2^2(t-1) \end{bmatrix} \quad (7)$$

and $r(t)$ represents a zero-mean residual term. The above model

makes use of the fact that, among different bed temperatures, the hot spot temperature has the strongest correlation with the product composition [Jutan et al., 1977]. The part that cannot be represented by the hot spot temperature is correlated with the input variables.

Using the output equation of Eqs. (5), (6) can be rearranged to

$$y_{MA}(t) = F_1 C z(t) + F_2 u(t-1) + F_3 u^2(t-1) + F_1 w(t) + r(t). \quad (8)$$

Eqs. (5) and (8) can be augmented to a single state space model as follows:

$$\begin{aligned} x(t+1) &= \bar{A}x(t) + \bar{B}u(t) + \bar{v}(t) \\ y(t) &= \bar{C}[u(t-1)]x(t) + \bar{w}(t) \end{aligned} \quad (9)$$

where

$$\begin{aligned} x(t) &\triangleq \begin{bmatrix} z(t) \\ u(t-1) \end{bmatrix}, y(t) \triangleq \begin{bmatrix} y_r(t) \\ y_{MA}(t) \end{bmatrix}, \bar{w}(t) \triangleq \begin{bmatrix} w(t) \\ F_1 w(t) + r(t) \end{bmatrix}, \bar{v}(t) \triangleq \begin{bmatrix} v(t) \\ 0 \end{bmatrix}, \\ \bar{A} &\triangleq \begin{bmatrix} A & 0 \\ 0 & I \end{bmatrix}, \bar{B} \triangleq \begin{bmatrix} B \\ I \end{bmatrix}, \bar{C}[u(t-1)] \triangleq \begin{bmatrix} C & 0 \\ F_1 C F_2 + F_3 U(t-1) \end{bmatrix}, \\ U(t) &\triangleq \begin{bmatrix} u_1^2(t) & 0 \\ 0 & u_2^2(t) \end{bmatrix}. \end{aligned}$$

Measurement of $y_{MA}(t)$, say $y_{MA}^m(t)$, is obtained with a long analysis delay. If the analysis takes d sampling times,

$$\begin{aligned} y_{MA}^m(t) &= F_1 C z(t-d) + F_2 u(t-d-1) + F_3 u^2(t-d-1) + e(t) \\ &= [F_1 C F_2 + F_3 U(t-d-1)]x(t-d) + e(t) \end{aligned} \quad (10)$$

where $e(t) \triangleq F_1 w(t-d) + r(t-d) + n(t)$; $n(t)$ is the measurement error. To include the delayed state in the state space model, Eq. (9) need to be augmented as follows:

$$\begin{bmatrix} x(t+1) \\ x_1(t+1) \\ \vdots \\ x_d(t+1) \end{bmatrix} = \begin{bmatrix} \bar{A} & 0 & \dots & 0 \\ I & 0 & \dots & 0 \\ \vdots & \ddots & \ddots & \vdots \\ 0 & \dots & I & 0 \end{bmatrix} \begin{bmatrix} x(t) \\ x_1(t) \\ \vdots \\ x_d(t) \end{bmatrix} + \begin{bmatrix} \bar{B} \\ 0 \\ \vdots \\ 0 \end{bmatrix} u(t) + \begin{bmatrix} \bar{v}(t) \\ 0 \\ \vdots \\ 0 \end{bmatrix}. \quad (11)$$

The measurement equation has a time-varying structure because of the different sampling periods of the temperatures and the yield. When the temperature and the yield are measured at the same time, the measurement equation is given by

$$\begin{bmatrix} y_r(t) \\ y_{MA}^m(t) \end{bmatrix} = \begin{bmatrix} [C \ 0] & 0 & \dots & 0 \\ 0 & \dots & 0 & [F_1 C F_2 + F_3 U(t-d-1)] \end{bmatrix} \begin{bmatrix} x(t) \\ x_1(t) \\ \vdots \\ x_d(t) \end{bmatrix} + \begin{bmatrix} w(t) \\ e(t) \end{bmatrix}. \quad (12)$$

When only the hot spot temperature is measured, the measurement equation becomes

$$y_r(t) = [C \ 0] \begin{bmatrix} x(t) \\ x_1(t) \\ \vdots \\ x_d(t) \end{bmatrix} + w(t). \quad (13)$$

For simplicity, Eqs. (11) to (13) are rewritten as

$$\begin{aligned} \mathbf{x}(t+1) &= \mathbf{A}\mathbf{x}(t) + \mathbf{B}\mathbf{u}(t) + \mathbf{v}(t) \\ \mathbf{y}(t) &= \mathbf{C}(t)\mathbf{x}(t) + \mathbf{w}(t). \end{aligned} \quad (14)$$

The above linear state space model is an exact transformation of Eqs. (5) and (6) without any approximation.

To include the integral action, we write Eq. (15) in the time-difference form [Lee et al., 1994].

$$\begin{aligned} \mathbf{x}(t+1) - \mathbf{x}(t) &= \mathbf{A}\{\mathbf{x}(t) - \mathbf{x}(t-1)\} + \mathbf{B}\{\mathbf{u}(t) - \mathbf{u}(t-1)\} + \mathbf{v}(t) - \mathbf{v}(t-1) \\ \mathbf{y}(t) - \mathbf{y}(t-1) &= \mathbf{C}(t)\mathbf{x}(t) - \mathbf{C}(t-1)\mathbf{x}(t-1) + \mathbf{w}(t) - \mathbf{w}(t-1). \end{aligned} \quad (15)$$

Here, we introduce an approximation of $\mathbf{C}(t-1) \approx \mathbf{C}(t)$ or equivalently $\mathbf{u}(t) \approx \mathbf{u}(t)$. Then the above can be rearranged to a state space model as follows:

$$\begin{aligned} \mathbf{z}(t+1) &= \Phi(t)\mathbf{z}(t) + \Gamma(t)\Delta\mathbf{u}(t) + \mathbf{n}(t) \\ \mathbf{y}(t) &= \Sigma(t)\mathbf{z}(t) \end{aligned} \quad (16)$$

where

$$\begin{aligned} \mathbf{z}(t) &\triangleq \begin{bmatrix} \Delta\mathbf{x}(t) \\ \mathbf{y}(t) \end{bmatrix}, \Phi(t) \triangleq \begin{bmatrix} \mathbf{A} & \mathbf{0} \\ \mathbf{C}(t)\mathbf{A} & \mathbf{I} \end{bmatrix}, \Gamma(t) \triangleq \begin{bmatrix} \mathbf{B} \\ \mathbf{C}(t)\mathbf{B} \end{bmatrix}, \Sigma(t) \triangleq \begin{bmatrix} \mathbf{0} & \mathbf{I}(t) \end{bmatrix}, \\ \mathbf{n}(t) &\triangleq \begin{bmatrix} \mathbf{v}(t) - \mathbf{v}(t-1) \\ \mathbf{w}(t+1) - \mathbf{w}(t) \end{bmatrix}, \Delta\mathbf{u}(t) \triangleq \mathbf{u}(t) - \mathbf{u}(t-1). \end{aligned}$$

2. State Estimator and Predictor Equation

The standard Kalman filter algorithm is used for state estimation [Åström and Wittenmark, 1997]

$$\begin{aligned} \mathbf{z}(t+1|t) &= \Phi(t)\mathbf{z}(t|t) + \Gamma(t)\Delta\mathbf{u}(t) \\ \mathbf{z}(t|t) &= \mathbf{z}(t|t-1) + \mathbf{K}(t)(\mathbf{y}(t) - \Sigma(t)\mathbf{z}(t|t-1)). \end{aligned} \quad (17)$$

where $\mathbf{K}(t)$ represents the Kalman gain.

The output prediction equation is easily constructed from (17) and given by

$$\begin{aligned} \mathbf{z}(t+k|t) &\approx \prod_{i=0}^{k-1} \Phi(t+i|t)\mathbf{z}(t|t) + \sum_{i=0}^{k-1} \Theta(t+i|t)\Gamma(t+i|t)\Delta\mathbf{u}(t+i) \\ \mathbf{y}(t+k|t) &= \Sigma(t+k)\mathbf{z}(t+k|t) \\ \Theta(t+i|t) &= \begin{cases} \prod_{j=i+1}^{k-1} \Phi(t+k-j|t) & \text{when } 0 \leq i < k-1 \\ \mathbf{I} & \text{when } i = k-1 \end{cases} \end{aligned} \quad (18)$$

where $\Phi(t+i|t)$ is an approximation of $\Phi(t+i)$ based on time t . In the formulation of $\Phi(t+i)$, the input values at time $t+i-d-1$ is needed. The future input values used in $\Phi(t+i)$ are approximated by $\mathbf{u}(t-1)$ when $i > d+1$ for simplicity. Likewise, $\Gamma(t+i|t)$ and $\Theta(t+i|t)$ are approximated by the same procedure. The reason for this approximation is to write the output prediction as a linear function of future input movements. By this approximation, the input is obtained by solving a quadratic programming problem. To mitigate potential prediction error by the above mentioned approximation, however, it is recommended to suppress excessive future input movements by imposing constraints on the input change and/or a more penalty on larger input change using \mathbf{R} in Eq. (19).

3. Input Calculation

When linear constraints are imposed on the process variables, we solve the following predictive control problem at every t and implement $\Delta\mathbf{u}_k(t)$ in the process:

$$\min_{\Delta\mathbf{u}_k(t)} \frac{1}{2} \left\{ \sum_{k=1}^p \|\mathbf{y}(t+k|t) - \mathbf{y}_d(t)\|_Q^2 + \|\xi(t+k)\|_S^2 + \sum_{k=1}^m \|\Delta\mathbf{u}(t+k-1)\|_R^2 \right\}$$

subject to Eq. (18) and linear constraints on the input and output variables

Here, $\xi(t+k)$ is a slack variable to relax the potential infeasibility of the output constraints [Zafiriou and Chiou, 1993]; $\mathbf{y}(t+k|t)$ represents the optimal prediction of $\mathbf{y}(t+k)$ based on the information up to t .

NUMERICAL SIMULATION

1. Model Identification

The identification experiment was conducted by applying independent PRTS (Pseudo Random Tertiary Sequence)'s to the two input variables. The state space model in Eq. (5) for the hot spot temperature was determined using a subspace identification method, called N4SID [Overschee and Moor, 1994]. The order of the obtained state space model was found to be 4. Also the nonlinear quality inferential model in Eq. (6) was found through the plain least squares method.

2. Results and Discussion

Numerical simulation has been performed for three cases. The first is on regulation when the inlet n-C4 concentration is decreased

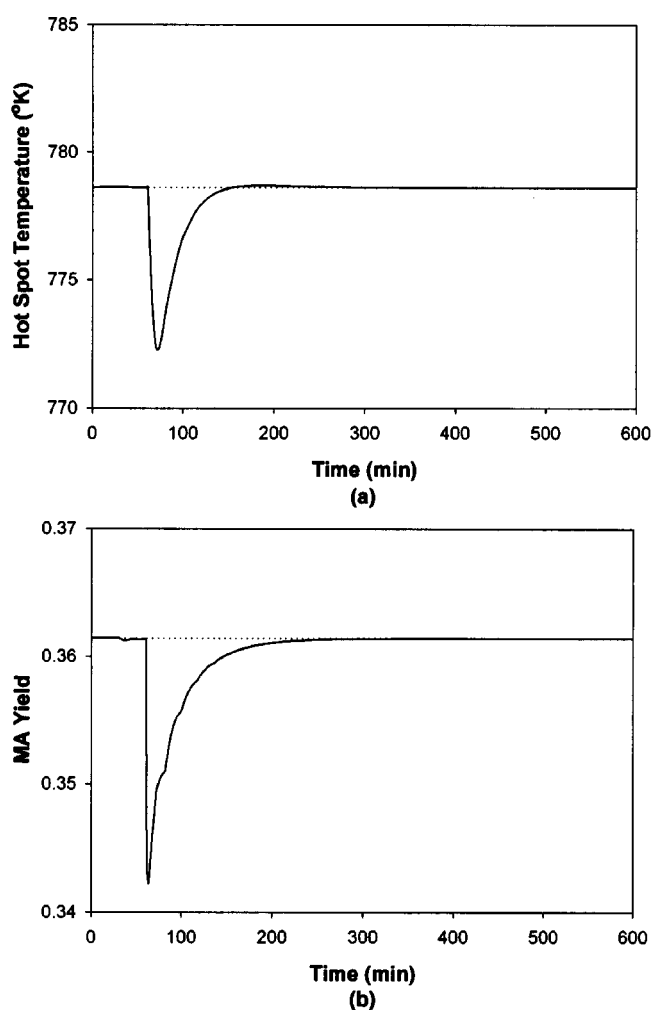


Fig. 5. Regulation performance of the proposed nonlinear inferential MPC technique for 5% decrease in the n-C4 concentration; (a) hot spot temperature, (b) MA yield.

by 5%. The second and third are on tracking when the set points of both hot spot temperature and MA yield are changed. For the second case, the new steady state is given in a region that can be linearly extended from the initial steady state. For the third case, however, the new steady state is given beyond the linear region. For each case, performance of proposed nonlinear inferential control is compared with that of linear inferential control.

Fig. 5 shows regulation performance of the proposed control technique when the inlet n-C4 concentration is decreased by 5% step-wise at 60 min. As can be seen, both hot spot temperature and MA yield are influenced by the unknown disturbance but recovered quickly by the proposed controller. Performance of linear inferential MPC is similar to Fig. 5 and is not shown here.

In Fig. 6, tracking performance of the proposed control technique is given when the set points of hot spot temperature and MA yield are raised by 5 °K and 4%, respectively. Both controlled variables converge to their new set points fast and smoothly. To this set point change, linear inferential MPC responds similarly and the result is not shown here.

The new steady state defined by the set point change in Fig. 6 is in fact in a linear region around the initial steady state. To show this,

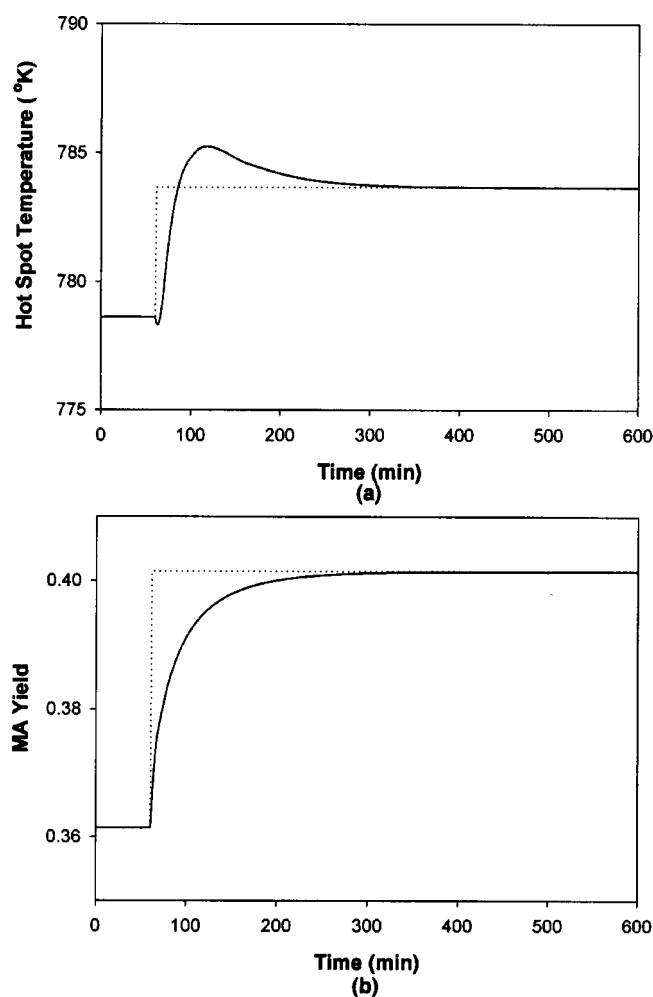


Fig. 6. Tracking performance of the proposed nonlinear inferential MPC technique for small changes in set points; (a) hot spot temperature, (b) MA yield.

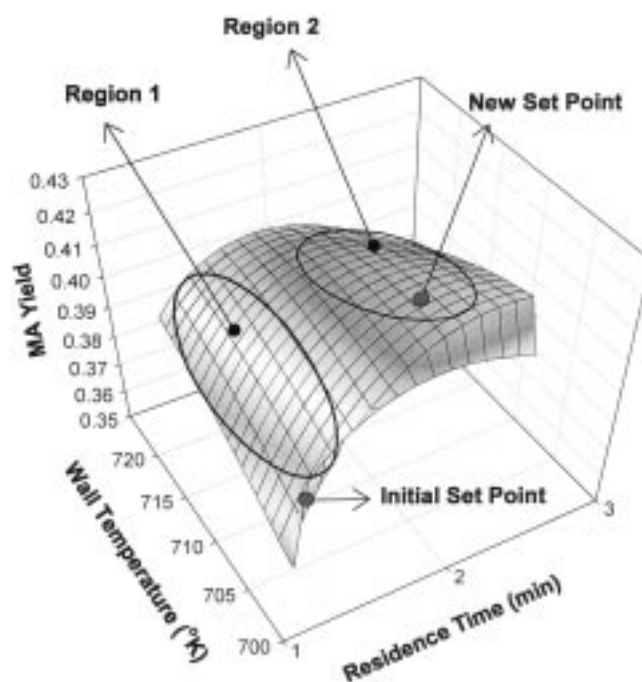


Fig. 7. Three dimensional plot of the steady state MA yield with respect of the input variables.

steady state MA yield is computed for various input values and plotted in Fig. 7. We can see that the new steady state is in the same uphill of the three dimensional plot. If the new steady state is given in *region 2*, i.e. on the other side of the hill or on the ridge of the hill, linear inferential MPC might not successfully function while the proposed nonlinear inferential MPC may still work.

To verify the above consideration, in the third case, we have tried the MA yield set point at 0.42 while the hot spot set point is given at 800 °K. Here, MA yield of 0.42 is not an achievable one as is manifested in Fig. 7. According to the objective in Eq. (19), if appropriately works, the controller will steer $y(t)$ to a maximum achievable point driving the hot spot temperature as closely as to its set point at the same time. Since the maximum achievable MA yield is around the ridge of Fig. 7, linear inferential MPC may not succeed to attain it. Fig. 8 summarizes the performance of linear inferential MPC. As can be observed, control fails leading to hot spot run-away and complete oxidation of n-C4. On the other hand, nonlinear inferential MPC works successfully as in given in Fig. 9. After some transient, MA yield and hot spot temperature settle at a new steady state near the dictated set points with some offsets.

CONCLUSIONS

Through this study, we have proposed a model predictive control (MPC) technique for a fixed-bed reactor where nonlinear quality inferential control with analysis delay is combined. A novel feature of this technique is that nonlinear behavior of the product quality can be incorporated in the inferential control without increasing any computational demand from the standard linear inferential MPC. Along with this study, problems with the bed-temperature measurement at a fixed position are discussed and a simple but useful technique to pursue the true hot spot temperature is proposed.

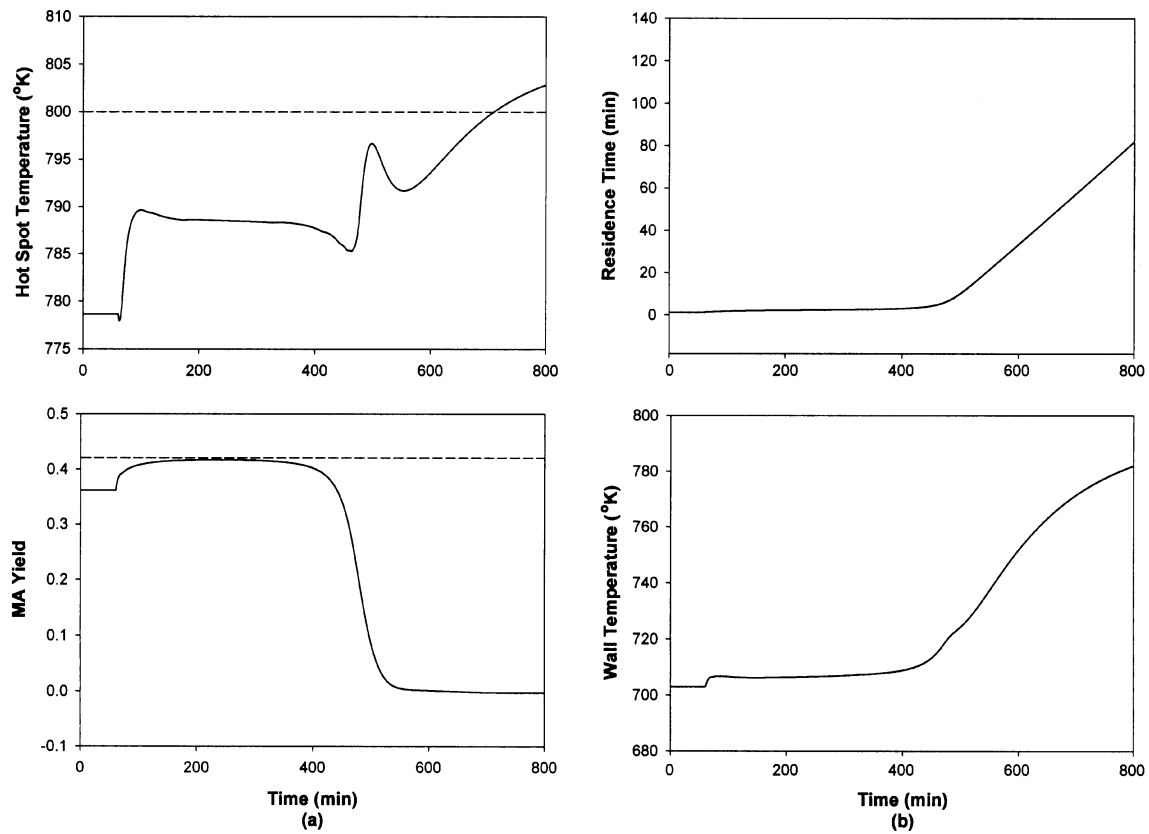


Fig. 8. Tracking performance of the linear inferential MPC technique for large changes in set points; (a) outputs, (b) inputs.

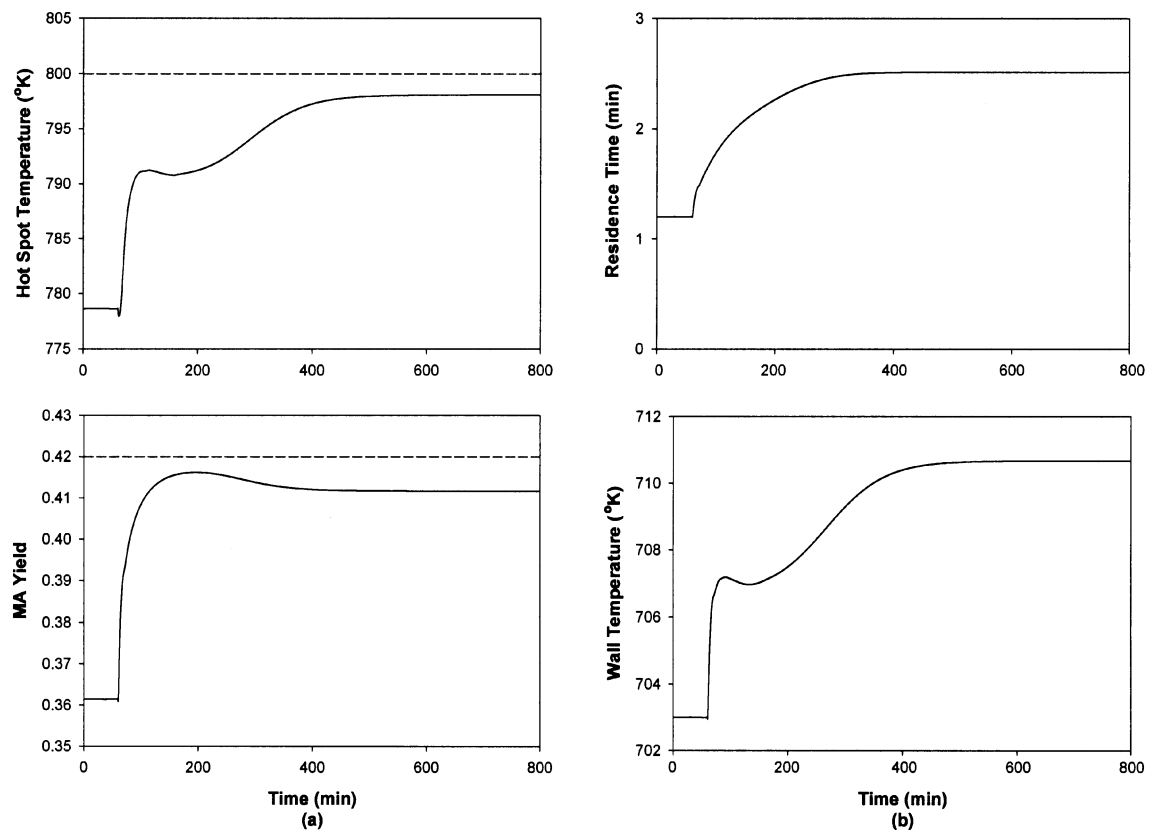


Fig. 9. Tracking performance of the proposed nonlinear inferential MPC technique for large changes in set points; (a) outputs, (b) inputs.

The proposed nonlinear inferential MPC technique has been applied to a non-adiabatic fixed-bed reactor where partial oxidation of n-butane to maleic anhydride takes place. Through a series of simulation studies, it was obviously seen that the proposed nonlinear inferential MPC technique can appropriately work over a wide region of operating condition while conventional linear inferential MPC can perform only in a narrow region where the reactor behavior can be approximated by a linear model. Also the proposed nonlinear inferential MPC technique can truly extremize the product yield or the operation profit if suitably modified.

ACKNOWLEDGEMENTS

The third author would like to acknowledge the financial support from Korea Ministry of Education through the Brain Korea 21 Project.

NOMENCLATURE

| | |
|---------------|---|
| L | : normalization factor for reactor length [cm] |
| R | : normalization factor for reactor diameter [cm] |
| T_R | : reference temperature for reactor temperature [$^{\circ}\text{K}$] |
| t | : reference residence time [sec] |
| T_w | : reference temperature for reactor wall temperature [$^{\circ}\text{K}$] |
| C_R | : reference concentration [mol] |
| k_{10} | : pre-exponential factor [$\text{cm}^3/\text{sec} \cdot \text{gcat}$] |
| k_{20} | : pre-exponential factor [$\text{cm}^3/\text{sec} \cdot \text{gcat}$] |
| k_{30} | : pre-exponential factor [$\text{cm}^3/\text{sec} \cdot \text{gcat}$] |
| Δh_1 | : heat of reaction [Kcal/gmol] |
| Δh_2 | : heat of reaction [Kcal/gmol] |
| Δh_3 | : heat of reaction [Kcal/gmol] |
| C_{pg} | : specific heat of reactant gas [cal/g $^{\circ}\text{K}$] |
| D_{er} | : effective radial diffusivity [cm^2/sec] |
| k_{er} | : effective radial conductivity [g/ cm^3] |
| \bar{C} | : mean specific hat defined by $C_{ps}\rho_B + C_{pg}\rho_g$ [cal/ $\text{cm}^3 \cdot ^{\circ}\text{K}$] |
| ε | : void factor |
| ρ_B | : bulk density [g/ cm^3] |
| ρ_g | : density of gas [g/ cm^3] |

REFERENCES

Åström, K. J. and Wittenmark, B., "Computer Controlled Systems,

- Theory and Design," 3rd ed., Prentice-Hall, N. J. (1997).
- Budman, H. M., Webb, C., Holcomb, T. R. and Morari, M., "Robust Inferential Control for a Packed-bed Reactor," *Ind. Eng. Chem. Res.*, **31**, 1665 (1992).
- Chen, C. and Sun, C., "Adaptive Inferential Control of Packed-bed Reactors," *Chem. Eng. Sci.*, **46**(4), 1041 (1991).
- Cho, C. K., Chang, K. S. and Cale, T. S., "Thermal Runaway Prevention in Catalytic Packed-bed Reactor by Solid Temperature Measurement and Control," *Korean J. Chem. Eng.*, **10**, 195 (1993).
- Doyle, F. J., Budman, H. M. and Morari, M., "Linearizing Controller Design for a Packed-bed Reactor Using a Low-order Wave Propagation Model," *Ind. Eng. Chem. Res.*, **35**, 3567 (1996).
- Froment, G. F. and Bischoff, K. B., "Chemical Reactor Analysis & Design," John Wiley & Sons (1979).
- Hua, X. and Jutan, A., "Nonlinear Inferential Cascade Control of Exothermic Fixed-bed Reactors," *AIChE J.*, **46**(5), 980 (2000).
- Hua, X., Mangold, M., Lienle, A. and Gilles, E. D., "State Profile Estimation of an Autothermal Periodic Fixed-bed Reactor," *Chem. Eng. Sci.*, **53**, 47 (1998).
- Jutan, A., Tremblay, J. P., Macgregor, J. F. and Wright, J. D., "Multi-variable Computer Control of a Butane Hydrogenolysis Reactor: Part I, II, and III," *AIChE J.*, **23**(5), 732 (1977).
- Kozub, D. J., Macgregor, J. F. and Wright, J. D., "Application of LQ and IMC Controllers to a Packed-bed Reactor," *AIChE J.*, **33**(9), 1496 (1987).
- Lee, J. H., Morari, M. and Garcia, C. E., "State-space Interpretation of Model Predictive Control," *AUTOMATICA*, **30**, 707 (1994).
- Lee, K. S., "Design of Computer Control System for a Non-adiabatic Fixed-bed Reactor," Ph.D. Thesis, Korea Advanced Institute of Science and Technology (1983).
- Lee, K. S. and Lee, W.-K., "On-line Optimizing Control of a Nonadiabatic Fixed Bed Reactor," *AIChE J.*, **31**(4), 667 (1985).
- Overschee, P. V. and Moor, B. D., "N4SID: Subspace Algorithms for the Identification of Combined Deterministic-Stochastic Systems," *AUTOMATICA*, **30**, 75 (1994).
- Zafiriou, E. and Chiou, H. W., "Output Constraint Softening for SISO Model Predictive Control," *Proc. of ACC.*, 372 (1993).